Albrecht et al., http://www.jcb.org/cgi/content/full/jcb.201406020/DC1

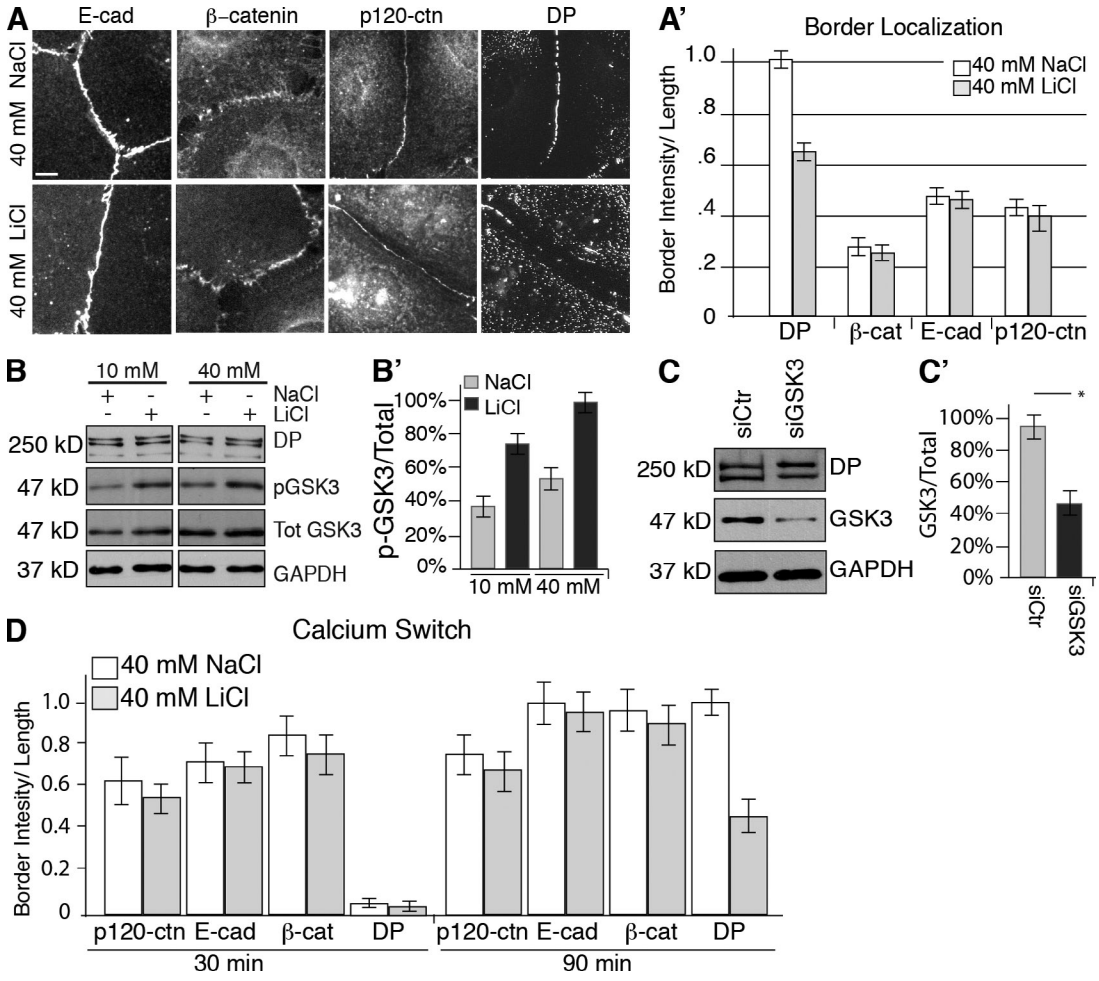

Figure S1. **Adherens junction assembly kinetics and localization are not affected by GSK3 inhibition.** (A) SCC9 cells treated with either NaCl and LiCl were fixed and stained with DP (NW6), E-cadherin (HECD-1), β-catenin (c2206), and p120-catenin and assessed by immunofluorescence. Bar, 10 µm. (A') Mean pixel intensities for p120catenin, E-cadherin, and DP were quantified along sites of cell–cell contact within the population (>10 fields and >40 borders analyzed). Error bars indicate SEM. (B and B') LiCl- and NaCl-treated SCC9s, assessed by immunoblotting. Densitometry quantification of three independent experiments. Error bars indicate SEM. (C and C') RIPA lysates of siCtr- and siGSK3-treated SCC9s, assessed by immunoblot probing for DP, pGSK3, total GSK3, and GAPDH. Densitometry quantification of three independent experiments; *, $P < 0.001$. Error bars indicate SEM. (D) Calcium switch analysis was performed to monitor adherens junction assembly during GSK3 inhibition. Cells were fixed after being in high calcium for 30 and 90 min and stained, as described in A. Mean pixel intensities for p120-catenin, E-cadherin, β-catenin, and DP were quantified along sites of cell–cell contact within the population (>10 fields and >40 borders). Quantified data are representative of three experiments. Error bars indicate SEM.

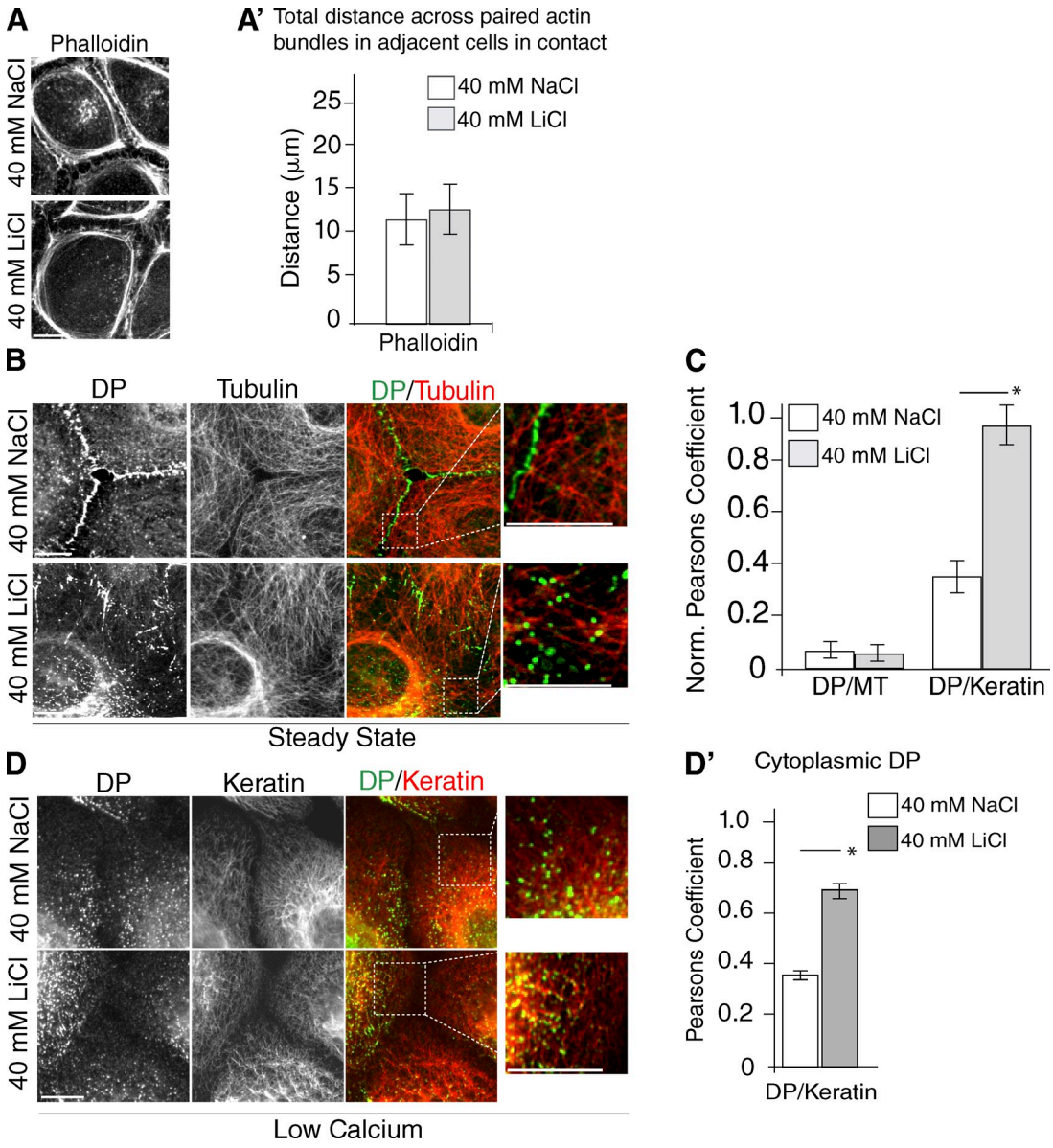

Figure S2. **GSK3 inhibition does not elicit global changes in cytoskeletal organization.** (A) NaCl and LiCl-treated SCC9 cells were stained with F-actin (phalloidin) and DP (NW6). Bar, 10 µm. The width of paired cortical actin bundles across adjacent cells was quantified as described previously (Godsel et al., 2010) and shown in A′ (includes the space between the bundles and the sum of the two bundles themselves in micrometers). Error bars indicate SEM. (B) NaCl- and LiCl-treated SCC9 cells were stained with tubulin (DM1α) and DP (NW6). Bars, 10 µm. (C) Quantification of Pearson's correlation coefficients for DP with MTs and DP with keratin in the same image were calculated from NaCl- and LiCl-treated SCC9 cells that were triple stained with tubulin (DM1α), DP (NW6), and keratin (K8; n = 20 image fields from three independent experiments, with >50 cytoplasmic regions calculated per condition). Error bars indicate SEM (*, $P < 0.001$). (D) NaCl or LiCl treatment of SCC9s incubated in low calcium media were fixed and stained with DP (NW6) and keratin (K8) antibodies. Bars, 10 µm. (D′) Pearson's correlation coefficients for DP and keratin were calculated using cytoplasmic regions. Representative region used for quantification is marked (white box). Data are representative of three experiments (*, $P < 0.0001$). Error bars indicate SEM.

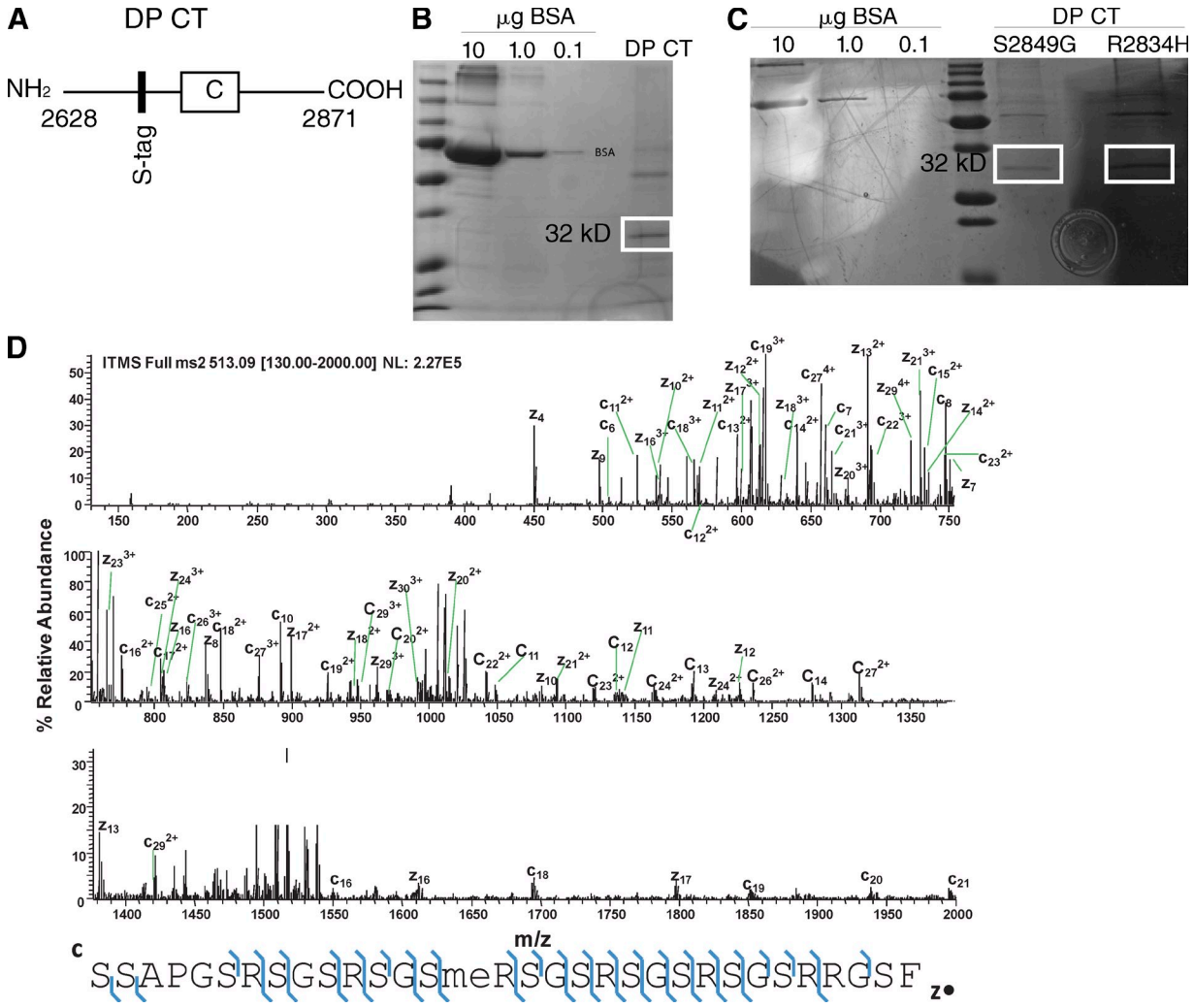

Figure S3. **Mass spectrometry analysis of DP S-tag protein expressed in HEK 293 cells.** (A) DP S-tag C-terminal truncation (DP CT; residues 2628–2871). (B) Coomassie-stained SDS-PAGE gel of WT DP S-tag expressed and purified from HEK 293 cells is assessed relative to 10 μg, 1 μg, and 0.1 μg of BSA protein for determination of DP S-tag (DP CT) protein concentration. (C) S2849G and R2834H DP S-tag (DP CT) proteins expressed and purified from HEK 293 cells were analyzed by Coomassie blue stain after SDS-PAGE. (D) FETD MS/MS identified arginine methylation of residues 2826, 2834, 2838, and 2846 from WT DP S-tag purified from HEK 293 cells. ETD tandem mass spectrum obtained from a precursor ion with an m/z of 513.09 (+6) corresponded to a peptide spanning residues 2628–2871 of DP S-tag (theoretical monoisotopic mass, 3072.5139; measured mass error, 1.09 ppm). The observed sequence ions are labeled in the figure and over the sequence. Masses of the N-terminal fragment ions from c_{15} to c_{29} show a shift of 28 D relative to the calculated masses of these product ions for the nonmodified peptide. C-terminal fragment ions from z_{17} to z_{30} are shifted 28 D. This is congruent with Arg2834 being dimethylated in this peptide.

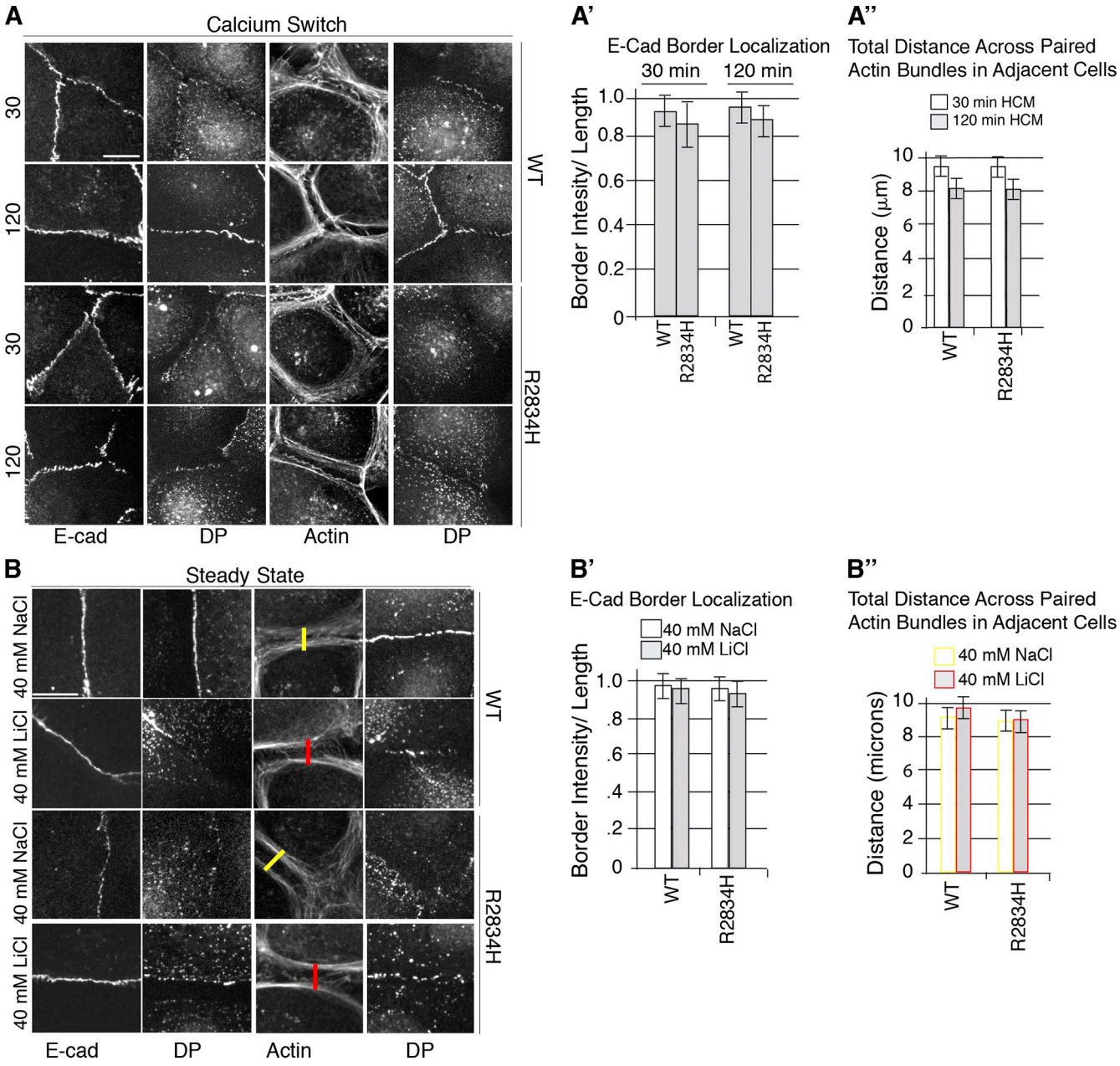

Figure S4. **Adherens junctions and actin cytoskeletal dynamics in DP-GFP stable cell lines. (A)** WT and R2834H DP-GFP SCC9 stable cell lines were fixed at 30 and 120 min after a calcium switch and stained with E-cadherin (HECD-1) and F-actin (phalloidin). Bar, 10 µm. (A′) Mean pixel intensities for E-cadherin and DP were quantified along sites of cell–cell contact within the population. Images were captured from >10 fields and >40 borders from three independent experiments. Error bars indicate SEM. (A″) The width of paired cortical actin bundles across adjacent cells were measured and compared between stable lines. Images were captured from >30 fields and >50 borders from three independent experiments. Error bars indicate SEM. (B) WT and R2834H DP-GFP stable cell lines were treated with NaCl or LiCl and stained with E-cadherin (HECD-1) and F-actin (phalloidin). Bar, 10 µm. (B′) Mean pixel intensities for E-cadherin and DP were quantified along sites of cell–cell contact within the population. Images were captured from >10 fields and >40 borders from three independent experiments. Error bars indicate SEM. (B″) The width of paired cortical actin bundles across adjacent cells were measured and compared between stable lines. Yellow and red bars denote widths calculated for NaCl- and LiCl-treated cells, respectively. Images were captured from >30 fields and >50 borders from three independent experiments. Error bars indicate SEM.

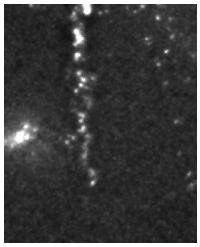

Video 1. **NaCl-treated SCC9 cells expressing WT DP-GFP.** Monolayers of SCC9 cells stably expressing WT DP-GFP (Godsel et al., 2005) were subjected to scratch wounding, treated with 40 mM NaCl, and imaged at 2-min intervals with five 0.5-µm z-stacks (80 min). Images were analyzed by time-lapse confocal microscopy using an inverted microscope (DMI6000; Leica) and are shown as multiimage projections at 10 frames/s (fps). The formation of cell–cell contacts is observed with DP precursor particles (yellow circles) incorporating into cell borders. Video corresponds to still frames in Fig. 1 H.

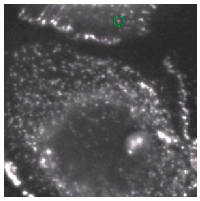

Video 2. **LiCl-treated SCC9 cells expressing WT DP-GFP.** Monolayers of SCC9 cells stably expressing WT DP-GFP were subjected to scratch wounding, treated with 40 mM LiCl, and imaged at 2-min intervals with five 0.5-µm z-stacks (80 min). Images were analyzed by time-lapse confocal microscopy using an inverted microscope (DMI6000; Leica) and are shown as multiimage projections at 10 fps. Yellow circle marks a DP particle appearing within the cytoplasm with delayed incorporation into the border. Green circle marks a representative example of a DP particle appearing within the cytoplasm that is unable to incorporate into borders during the 80 min that cells were imaged. Video corresponds to still frames in Fig. 1 H.

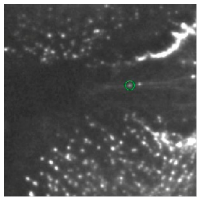

Video 3. **LiCl-treated SCC9 cells expressing WT DP-GFP.** Monolayers of SCC9 cells stably expressing WT DP-GFP were subjected to scratch wounding, treated with 40 mM LiCl, and imaged at 2-min intervals with five 0.5-µm z-stacks (80 min). Images were analyzed by time-lapse confocal microscopy using an inverted microscope (DMI6000; Leica) and are shown as multiimage projections at 10 fps. Green circles mark representative examples of DP particles appearing within the cytoplasm that is unable to incorporate into borders during the 80 min that cells were imaged. Video corresponds to still frames in Fig. 1 H′.

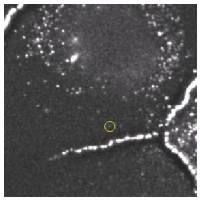

Video 4. **WT DP-GFP–expressing SCC9 cells during wound-healing assay.** Monolayers of SCC9 cells stably expressing WT DP-GFP (green) were subjected to scratch wounding and imaged at 2-min intervals with five 0.5-µm z-stacks (80 min). Images were analyzed by time-lapse confocal microscopy using an inverted microscope (DMI6000; Leica) and are shown as multiimage projections at 10 fps. DP precursors (yellow circles) are observed incorporating into nascent cell borders, as demonstrated previously (Godsel et al., 2005). Video corresponds to still frames in Fig. 4 E (rotated for display).

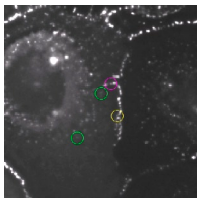

Video 5. **R2834H DP-GFP–expressing SCC9 cells during wound-healing assay.** Monolayers of SCC9 cells stably expressing R2834H DP-GFP were subjected to scratch wounding and imaged at 2-min intervals with five 0.5-µm z-stacks (80 min). Images were analyzed by time-lapse confocal microscopy using an inverted microscope (DMI6000; Leica) and are shown as multiimage projections at 10 fps. Purple circles depict DP particles with delayed trafficking kinetics that eventually incorporate into junctions and green circles denote DP particles that remain stuck within the cytoplasm. Yellow circles highlight representative examples of DP precursors that are observed incorporating into nascent cell borders. Video corresponds to still frames in Fig. 4 E.

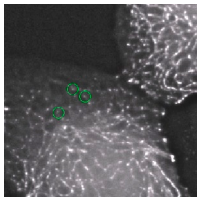

Video 6. **S2849G DP-GFP–expressing SCC9 cells during wound-healing assay.** Monolayers of SCC9 cells stably expressing S2849G DP-GFP (Godsel et al., 2005) were subjected to scratch wounding and imaged at 2-min intervals with five 0.5-µm z-stacks (80 min). Images were analyzed by time-lapse confocal microscopy using an inverted microscope (DMI6000; Leica) and are shown as multiimage projections at 10 fps. Cell borders form with delayed assembly as previously demonstrated (Godsel et al., 2005). Green circles mark DP precursors that appear within the cytoplasm and do not incorporate into junctions. Video corresponds to still frames in Fig. 4 E.

Table S1. **Six novel phosphorylated serine sites in the DP C-tail**

DP S-Tag	Peptide sequence	Phosphosites
WT	SSAPGSRSGSRSGpSRSGSRSGSRSGSRRGSF	Ser2833
	SSAPGSRSGSRSGSRSGpSRSGSRSGSRRGSF	Ser2837
	SSAPGSRSGSRSGSRSGSRpSGSRSGSRRGSF	Ser2839
	SSAPGSRSGSRSGSRSGSRSGpSRSGSRRGSF	Ser2841
	SSAPGSRSGSRSGSRSGSRSGSRpSGSRRGSF	Ser2843
	SSAPGSRSGSRSGSRSGSRSGSRSGpSRRGSF	Ser2845
	SSAPGSRSGSRSGSRSGSRSGSRSGSRRGpSF	Ser2849
	SSAPGSRSGSRSGpSRSGSRSGSRSGSRRGpSF	Ser2833 and 2849
	SSAPGSRSGSRSGSRSGpSRSGSRSGSRRGpSF	Ser2839 and 2849
S2849G	SSAPGSRSGSRSGSRSGSRSGSRSGSRRGGF	–
R2834H	SSAPGSRSGSRSGSHSGSRSGSRSGSRRGpSF	Ser2849

FETD MS/MS identified novel phosphorylation sites at serine residues 2833, 2837, 2839, 2841, 2843, and 2845 from WT DP S-tag protein purified from HEK 293 cells. Serine residues were phosphorylated simultaneously at 2833 and 2849 and also at 2839 and 2849. Phosphorylation at Ser2849 confirmed previous mass spectrometry screens that identified this site. S2849G DP S-tag purified from HEK 293 cells ablates phosphorylation at all sites within this peptide. R2834H DP S-tag purified from HEK 293 cells retains phosphorylation at a single site at Ser2849 within this peptide.

Table S2. **Four novel arginine methylation sites are identified in the DP C-tail**

Peptide sequence	PTM sites
SSAPGSmeRSGSRSGSRSGSRSGSRSGSRRGSF	Arg2826
SSAPGSRSGSRSGSmeRSGSRSGSRSGSRRGSF	Arg2834
SSAPGSRSGSRSGSRSGSmeRSGSRSGSRRGSF	Arg2838
SSAPGSRSGSRSGSRSGSRSGSRSGSmeRRGSF	Arg2846
SSAPGSRSGSRSGSmeRSGSRSGpSRSGSRRGSF	Arg2834 and Ser2841
SSAPGSmeRSGSRSGSmeRSGSRSGpSRSGSRRGSF	Arg2826, Arg2834, and Ser2841
SSAPGSRSGSRSGSmeRSGSRSGSRpSGSRRGSF	Arg2834 and Ser2843
SSAPGSRSGSRSGSmeRSGSmeRSGSRpSGSRRGSF	Arg2834, Arg2838, and Ser2843

FETD MS/MS identified arginine methylation of residues 2826, 2834, 2838, and 2846 from DP S-tag purified from HEK 293 cells. Among these spectra, arginine methylation occurred simultaneously with serine phosphorylation with residues Arg2834 and Ser2841, Arg2826 and 2834 and Ser2841, Arg2834 and Ser2843, and Arg2834 and 2838 and Ser2843.

References

Godsel, L.M., S.N. Hsieh, E.V. Amargo, A.E. Bass, L.T. Pascoe-McGillicuddy, A.C. Huen, M.E. Thorne, C.A. Gaudry, J.K. Park, K. Myung, et al. 2005. Desmoplakin assembly dynamics in four dimensions: multiple phases differentially regulated by intermediate filaments and actin. *J. Cell Biol.* 171:1045–1059. http://dx.doi.org/10.1083/jcb.200510038

Godsel, L.M., A.D. Dubash, A.E. Bass-Zubek, E.V. Amargo, J.L. Klessner, R.P. Hobbs, X. Chen, and K.J. Green. 2010. Plakophilin 2 couples actomyosin remodeling to desmosomal plaque assembly via RhoA. *Mol. Biol. Cell*. 21:2844–2859. http://dx.doi.org/10.1091/mbc.E10-02-0131